JOURNAL OF AIRCRAFT
Vol. 41, No. 3, May–June 2004

Strength Analysis of Ceramics Under Different Constraints by Movable Cellular Automata Method

Ke Chen*
Nanjing University of Science and Technology, 210094 Nanjing, People's Republic of China
Dewu Huang†
Shenyang Institute of Technology, 110015 Shenyang, People's Republic of China
and
E. V. Shilko‡ and S. G. Psakhie§
Russian Academy of Sciences, 634021, Tomsk, Russia

In this paper the movable-cellular-automata (MCA) method was applied to study the features of the fracture process and strength properties of ceramics specimen under different constraint conditions. Results of calculations showed that mechanism of fracture of ceramic materials is dependent on the surroundings or contact conditions. It is demonstrated that the MCA method has been successfully used for modeling fracture of the different types of materials and structures.

Introduction

CERAMICS materials are now used to make some parts of aircraft construction, and one of the main problems of these parts is in increasing of the structure's viability under dynamic loading. As far as real collision experiments of the complex structures are sufficiently expensive and getting of detailed information is often difficult, the methods of computer-aided study are considered as one of the tools to solve the problems.[1,2]

In this paper a new mode of material optimization is suggested, which is based on the influence of surrounding and contact parts. In accordance with the discrete concept, the movable-cellular automata (MCA) has been successfully served for simulation of the fractures and damages of different materials on the various constraints.[3,4]

Concept of MCA Method

The discrete computational mechanics nowadays was mainly developed as molecular dynamics at the atomic level. The molecular dynamics has found remarkably wide application in a great number of fields of modern science, from physics to biology. For the last 15–20 years it has been marked that the particle method was used to describe different media including granular and loose materials.[5–15]

Within the framework of the method of MCA,[16–20] a system to be simulated is an ensemble of interacting automata (elements) of finite size.[4] The concept of the MCA method is based on the introduction of a new type of state, namely, the state of a pair of automata. This has made possible the coming up to a space variable and using it as a parameter of switching. The overlapping of a pair of automata was chosen as such a parameter (Fig. 1):

$$h^{ij} = r^{ij} - r_0^{ij} \tag{1}$$

In the simplest case there are two states of pairs:

Linked state:

$$h^{ij} < h_{\max}^{ij} \tag{2}$$

Unlinked state:

$$h^{ij} > h_{\max}^{ij} \tag{3}$$

In this case the linked state is indicative of chemical bonds between elements, and the unlinked state indicates that there is no chemical bond between automata. This parameter is of space dimension. This fact results in a qualitatively new property of automata, that is, in the capability of changing their positions in space and, consequently, changing the spatial arrangement of the whole system. Thus, the change in the state of the pairs of automata is governed by relative displacements of automata forming a pair. From relations (2) and (3) the medium constituted by such pairs can be considered as a bistable medium.

The state of a pair of automata ij is uniquely determined by two types of fields $h^{\alpha\beta}(t)$. The first type is associated with the state of the pair itself $ij - h^{ij}(t)$, and the second is associated with the states of its neighboring pairs $\{ik\} - h^{ik}$ and $\{jl\} - h^{jl}$ (see Fig. 2). These fields essentially define local deformations (deformation of elements of the medium) and, consequently, the distribution and fluxes elastic energy in the simulated medium.

The time derivative $\dot{h}^{ij}(t)$ can be determined following the Viner–Rothenblute model.[18] In this case the active bistable medium under study can be described by the equation

$$\frac{\Delta h^{ij}}{\Delta t} = f(h^{ij}) + \sum_{k \neq j} C(ij, ik) I(h^{ik}) + \sum_{l \neq i} C(ij, jl) I(h^{jl}) \tag{4}$$

where the function $f(h^{ij})$ has the meaning of the relative velocity of automata (V^{ij}); $C[ij, ik(jl)]$ is the coefficient associated with the transfer of the parameter h from the pair ik (or jl) to the pair ij; $I[h^{ik(jl)}]$ is an explicit function of $h^{ik(jl)}$, which defines the redistribution of the parameters h^{ik} and h^{jl} between the pairs ij, ik, and jl. These parameters are shown in Fig. 2.

Within the linear approximation the function $I[h^{ik(jl)}]$ can be written as

$$I[h^{ik(jl)}] = \psi[\alpha_{ij,ik(jl)}] V_n^{i(k)[j(l)]} \tag{5}$$

In the general case the multiplier $\psi[a_{ij,ik(jl)}]$ is a combination of trigonometrical function, which is defined by the relative arrangement of the automata.

Received 7 October 2002; revision received 17 July 2003; accepted for publication 23 July 2003.

*Associate Professor, Institute of Mechanics Engineering; currently Associate Professor, Institute of Mechanics Engineering, Shenyang Institute of Technology, 110015 Shenyang, People's Republic of China.

†Professor, Institute of Mechanics Engineering, 117, Nanta Street, Dongling District; hdwcmh@sina.com.

‡Research Associate, CAD Laboratory, Institute of Strength Physics and Materials Science.

§Professor, Head of Institute of Strength Physics and Materials Science.

As mentioned in Eq. (1), the system consisting of movable cellular automata will be described by the translational equations of motion:

$$\frac{d^2h^{ij}}{dt^2} = \left(\frac{1}{m^i} + \frac{1}{m^j}\right)p^{ij} + \sum_{k\neq j} C(ij, ik)\psi(\alpha_{ij,ik})\frac{1}{m^i}p^{ik} + \sum_{l\neq i} C(ij, jl)\psi(\alpha_{ij,jl})\frac{1}{m^j}p^{jl} \quad (6)$$

To obtain Eq. (6), the term $(d/dt)V^{i(j)k(l)}$ was represented as $(1/m^i)p^{i(j)k(l)}$, where $p^{i(j)k(l)}$ is the force of interelement interaction. It is defined by the function of the interautomata response. The coefficient $C[ij, ik(jl)]$, as Eq. (4), is associated with the transfer of the parameter h from the pair ik (or jl) to the pair ij. The term $\psi(\alpha_{ij,ik})$ is determined by the Poisson ratio and, consequently, is related to the mutual arrangement of the pairs of elements ij and ik.

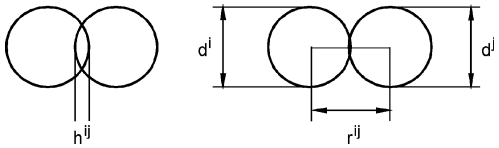

Fig. 1 h^{ij} **is the overlapping parameter;** r^{ij} **is the distance between the centers of neighboring automata,** $r_0^{ij} = (d^i + d^j)/2$**, where** d **is automaton size.**

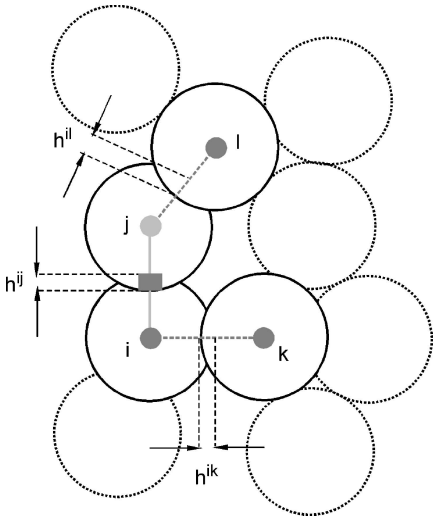

Fig. 2 Overlapping parameters for the pairs *ij*, *ik*, **and** *jl*.

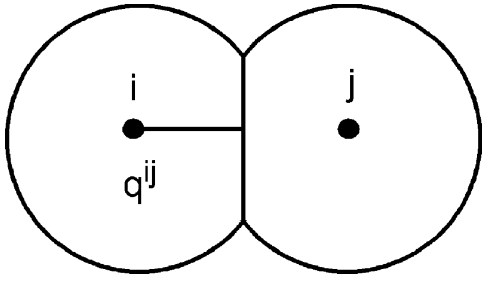

Fig. 3 Expression for calculation of the relative deformation of automata.

The equations of motion for rotation can be written similarly in the following form:

$$\frac{d^2\theta^{ij}}{dt^2} = \left(\frac{q^{ij}}{J^i} + \frac{q^{ji}}{J^j}\right)\tau^{ij} + \sum_{k\neq j} S(ij, ik)\frac{q^{ik}}{J^i}\tau^{ik} + \sum_{l\neq i} S(ij, jl)\frac{q^{jl}}{J^j}\tau^{jl} \quad (7)$$

Here θ^{ij} is the angle of the relative rotation of elements (it is also the switching parameter similar to h^{ij}); q^{ij} is the distance from the center of the automaton i to the point of contact line with the automaton j (moment arm, see Fig. 3); τ^{ij} is the tangential interaction of pairs; $S[ij, ik(jl)]$ are some coefficients associated with the transfer of the parameter θ from the pair ik (or jl) to the pair ij.

It can be seen well that if $C[ij, ik(jl)] = 1$ and $S[ij, ik(jl)] = 1$, Eqs. (6) and (7) are totally equivalent to the Newton–Euler equations of motion for many-particle interaction. As already noted, the term $C[ij, ik(jl)]$ determines the transfer of the parameter h from the pair ik (or jl) to the pair ij. The term elastic information means information on relative elastic displacements of elements, which is transferred to elastic fields. Hence, equations of motion (6) and (7) make it possible to allow for delays $\delta t^{ij(ik)}$ and $\delta t^{ij(il)}$ and effect of the overlapping parameter for the pairs $\{ik\}$ and $\{jl\}$ on the interaction of the pair of elements ij (Fig. 2).

For each automaton the notion of strain, relative deformation, ε^{ij} is introduced. The expression for calculation of ε^{ij} is presented in Fig. 3. The parameter q^{ij} is the distance from mass center of the automaton i to the point of its contact line with the automaton j. It is possible to set aside four basic types of the response function. In the simplest case the interautomata interaction is assumed elastic and linear. In this approximation the response function can be treated as a linear function of the overlapping parameter. In this case the loading and unloading follows the same curve. Response functions just mentioned can be used for simulating the process of fracture of brittle materials such as ceramics, concrete, etc., and constructions designed on the base of such materials.

Functions of response for irreversible behavior of materials like plastic deformation have to be fitted especially for each material with taking into consideration the conditions of loading.[3,4] The MCA method is allowed to simulate the processes of elastoplastic deformation and degradation at the meso- and microlevels depending on the type of response functions for movable automata.[16–20]

Description of Setup

We considered the behavior of ZrO_2-based ceramic specimens under uniaxial compression. Despite being simple, it is essential in analysis of fracture and damages of the brittle materials. Simulated specimens are two kinds of structures consisted of a ZrO_2 (5% porosity) ceramic material without constraint and a ZrO_2 (5% porosity) ceramic material with constraint conditions (steel ring and

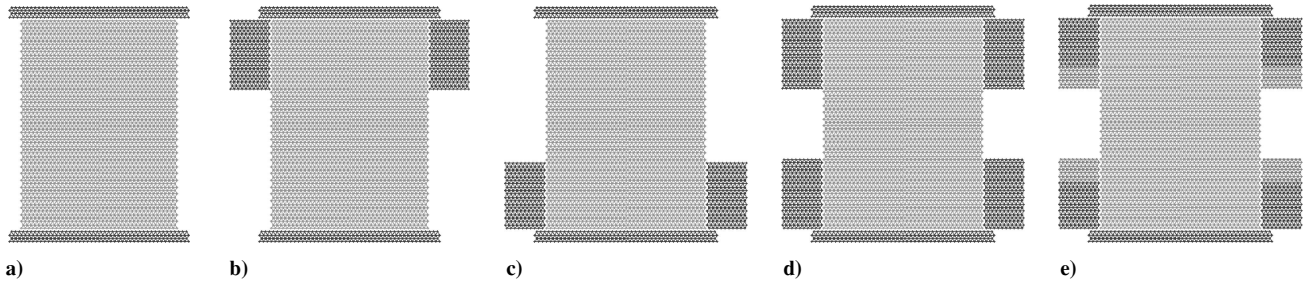

Fig. 4 Simulated setups: a) specimen with free side; b) specimen with steel ring at the top; c) specimen with steel ring at the bottom; d) specimen with steel rings at the top and bottom; and e) specimen with rings of different materials at the top and bottom.

complex materials ring). Constraint ring was placed at the top and bottom of the specimen. The ring was free in the Y direction (vertical direction), and its external surface was fixed in the X direction. The sizes of the simulated specimens are 1.35 cm × 1.05 cm (Fig. 4). To study the effect of the constraint ring, the complex materials of constraint ring are consisted of two kinds of materials, PM bronze and steel materials. In this paper of two dimensions, the automaton can be regarded as a circle clement, and its diameter was 0.25 mm.

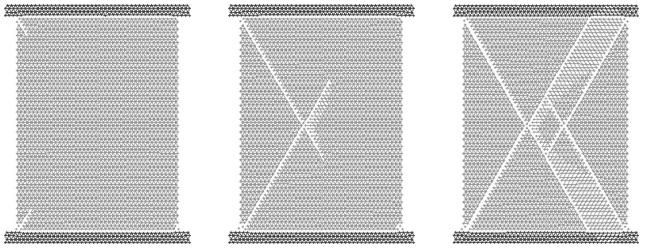

a) ε **= 1.21%** **b)** ε **= 1.23%** **c)** ε **= 1.26%**

Fig. 5 Main stages of fracture of base specimen (with free side).

Load was applied by setting up a constant velocity $V = 0.5$ m/s for the piston (upper plate in the Fig. 4). The supporting plate (bottom plate in Fig. 4) was unmovable.

Results and Discussion

Ceramics is typically a brittle material. When compressed by indenter with constant velocity $V = 0.5$ m/s, the stress concentration is very severe at the top/bottom of the specimen. So the macrocrack was initiated in the regions firstly (Fig. 5a). Here the strain is 0.0121, and this smaller value can be approximated as zero. Thus the basic specimen demonstrates pure brittle behavior.

We have researched the fracture behavior of ceramic materials under difference-constraint conditions. When the constraint ring was placed at the top or bottom separately, the strain of the automata in the X direction was limited in the region, and local stress increased. Initial crack did not generate at the corner of the ring (Figs. 6 and 7). The constraint ring increased the strength of the specimen. But fracture types of the specimens are brittle fracture obviously. The constraint ring changed the position of initial crack generation.

To take into account the double-constraint rings (Figs. 8, and 9). The material of the ring in the Fig. 8 was steel material; its Young's

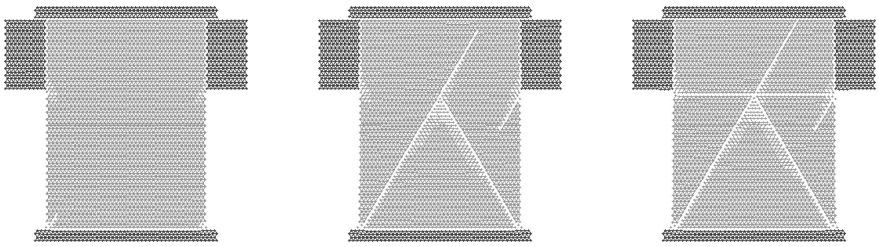

a) ε **= 1.08%** **b)** ε **= 1.12%** **c)** ε **= 1.16%**

Fig. 6 Main stages of fracture of the specimen with ring at the top.

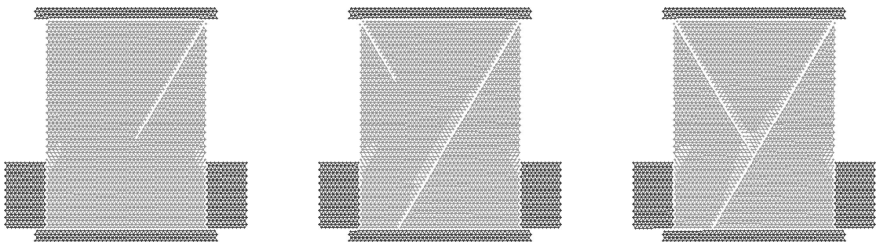

a) ε **= 1.1%** **b)** ε **= 1.12%** **c)** ε **= 1.14%**

Fig. 7 Main stages of fracture of the specimen with ring at the bottom.

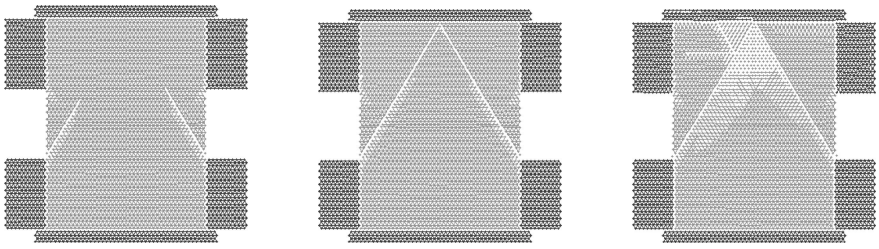

a) ε **= 0.97%** **b)** ε **= 1.04%** **c) 1.61%**

Fig. 8 Main stages of fracture of the specimen with rings at the top and bottom.

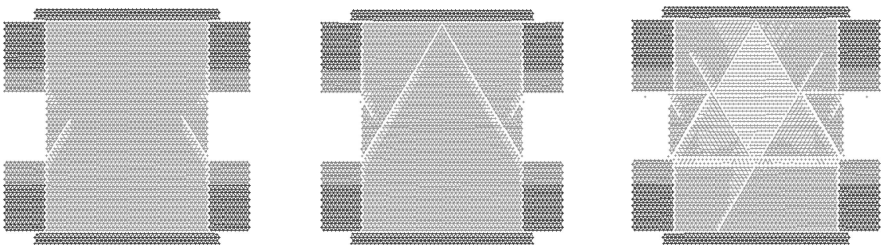

a) ε **= 1.10%** **b)** ε **= 1.14%** **c)** ε **= 1.61%**

Fig. 9 Main stages of fracture of the specimen with rings at the top and bottom.

modulus is 206 Gpa. Because of stress concentration, the initial cracks were produced at the corner of the steel rings (Fig. 8). In the Fig. 9 the two materials of the rings are PM bronze and steel. PM bronze is a kind of soft material, and its Young's modulus is 40 Gpa. Because double-constraint rings and difference of materials, the failure types are different. As a soft material, it diffused the stresses at the corner (Fig. 9).

In simple terms, the value of resistant force of specimens was calculated using the formulae $\sigma = F/S$, where F is loading force applied to the piston (equal to specimen resistant force) and S is the upper square of the ZrO_2 specimen. The value of specimen deformation was calculated using the formula $\varepsilon = D_y/H_0$, where D_y is displacement of the piston and H_0 is initial height of the specimen. Loading diagrams of five tested specimens are shown in the Fig. 10.

In Fig. 10 the square area under the plot represents the accumulation of crash energy absorbed in the specimen. The equation of crash momentum is $S = \sum_{i=1}^{N} (F_y^i \Delta t)$. So we get the result $S_2/S_1 = 1.44$. Here, S_1 and S_2 can be associated with crash momentum of the specimen with the free side and the specimen with rings that consist of PM bronze and steel materials at the top and bottom. The structure of the specimen with rings that consist of PM bronze and steel materials at the top and bottom has the better capability of shock absorption than the specimen with the free side. These results have been demonstrated in much practical engineering, and in fact, engineers and designers including the technicians in airplane building understand how to strengthen the mechanical parts with the possible different constraint conditions.

For Fig. 4e to simulate the strength of the specimens with constraint rings of different Young's modulus, results show (Fig. 11) that the soft material of a small Young's modulus can increase the specimen strength. When the Young's modulus of the soft material is 5 Gpa, the permissible maximum stress is 1284.88 Mpa; and when the Young's modulus is 200 Gpa, the permissible maximum stress is 940.16 Mpa. The curve is smooth and declines. This result has great significance in the structure design of the aircraft. In some cases to put the reasonable constraints on the structures can improve the properties of materials.

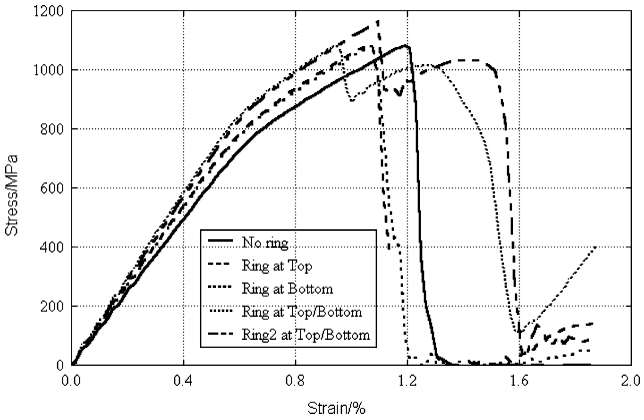

Fig. 10 Loading diagrams of five tested specimens.

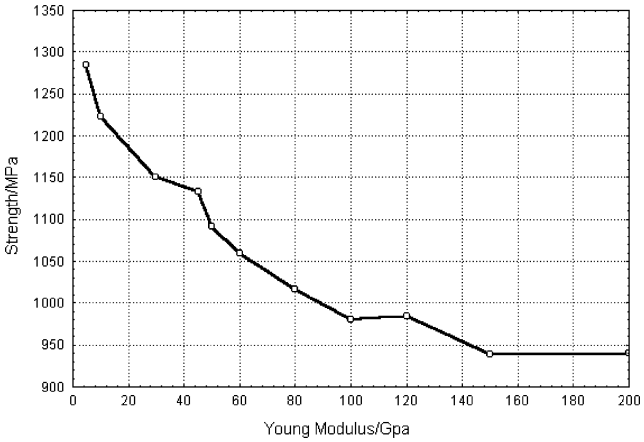

Fig. 11 Strength diagram of specimens with constraint materials of different Young's modulus.

Conclusions

In the present paper a new advanced movable-cellular-automata method has been applied to the investigation of the response and fracture of ZrO2 (5% porosity) ceramic material under different constraint conditions. Results of the simulation show that the strength properties of the specimen from engineering as well as from the research of materials science can be changed with transforming different constraint conditions. So, the performance of all engineering devices, structures, and constructions is dependent on constraint by the surrounding or contacting parts and materials used in practice.

References

[1]Panin, V. E., "Methodology of Physical Mesomechanics as the Basis for Model Construction of Computer-Aided Design of Materials," *Russian Physics*, Vol. 38, No. 11, 1995, pp. 1105–1115.

[2]Huang, D., Redekop, D., and Xu, B., "Natural Frequencies and Mode Shapes of Curved Pipes," *Computers and Structures*, Vol. 63, No. 3, 1997, pp. 465–473.

[3]Psakhie, S. G., Horie, Y., and Korostelev, S. Y., "Movable Cellular Automata Method as a Tool for Simulation Within the Framework of Physical Mesomechanics of Materials," *Russian Physics*, Vol. 38, No. 11, 1995, pp. 1001–1011.

[4]Psakhie, S. G., Horie, Y., and Ostermeyer, G. P., "Movable Cellular Automata Method for Simulating Materials with Mesostructure," *Theoretical and Applied Fracture Mechanics,* Vol. 37, No. 3, 2001, pp. 311–334.

[5]Cundall, P. A., and Strack, O. D. L., "A Discrete Numerical Model for Granular Assemblies," *Geotechnique,* Vol. 29, No. 1, 1979, pp. 47–54.

[6]Cundall, P. A., "A Computer Simulations of Dense Sphere Assembles," *Micromechanics of Granular Materials*, edited by M. Satake, and J. T. Jenkins, Elsevier, Amsterdam, 1988, pp. 213–223.

[7]Herrmann, H. J., "Simulating Granular Media on the Computer," *The 3rd Granada Lectures in Computational Physics*, edited by P. L. Garrido and J. Marro, Heidelberg, Springer, 1995, pp. 67–74.

[8]Hemmingsson, J., Herrmann, H. J., and Roux, S., "On Stress Networks in Granular Media," *Physics*, Vol. 7, 1997, pp. 291–298.

[9]Walton, O. R., "Numerical Simulation of Inclined Chute Flows of Monodisperse, Inelastic, Frictional Spheres," *Mechanics of Materials,* Vol. 16, No. 2, 1993, pp. 239–236.

[10]Walton, O. R., "Numerical Simulation of Inelastic, Frictional Particle-Particle Interaction," *Particulate Two-Phase Flow*, edited by M. C. Roco, Butterworth-Heinemann, Boston, 1993, pp. 884–902.

[11]Luding, S., "Granular Materials Under Vibration/Simulations of Rotating Spheres," *Physical Review E*, Vol. 52, No. 4, 1995, pp. 4442–4452.

[12]Poschel, T., "Granular Material Flowing down an Inclined Chute/A Molecular Dynamic Simulation," *Physics II*, Vol. 3, 1993, pp. 27–35.

[13]Greenspan, D., "Particle Modeling in Science and Technology, Coll. Math.," *Societatis Janos Bolyai*, Vol. 50, No. 1, 1988, pp. 51–60.

[14]Ostermeyer, G. P., "Mesoscopic Particle Method for Description of Thermomechanical and Friction Processes," *Physical Mesomechanics,* Vol. 2, No. 6, 1999, pp. 23–28.

[15]Hockney, R. W., and Eastwood, J. W., *Numerical Simulation by the Particle Method*, McGraw–Hill, New York, 1981, pp. 12–20.

[16]Psakhie, S. G., Korostelev, S. Y., and Smolin, A. Y., "Movable Cellular Automata Method as a Tool for Physical Mesomechanics of Materials," *Physical Mesomechanics,* Vol. 1, No. 1, 1998, pp. 89–101.

[17]Dmitriev, A. I., and Korostelev, S. Y., "Movable Cellular Automata Method as a Tool for Simulation at the Mesolevel, Proceedings of RAS.," *Mechanics of Solids*, Vol. 6, No. 1, 1999, pp. 87–96.

[18]Psakhie, S. G., and Ostermeyer, G., "Movable Cellular Automata Method as a New Tool in Computational Mechanics," *Computational Materials Science*, Vol. 16, No. 4, 1999, pp. 333–344.

[19]Psakhie, S. G., Dmitriev, A. I., and Shilko, E. V., "Method of Movable Cellular Automata as a New Trend of Discrete Computational Mechanics. I. Theoretical Description," *Physical Mesomechanics*, Vol. 3, No. 2, 2000, pp. 5–12.

[20]Chen, K., Xu, Y., and Huang, D. W., "Investigation of Fracture Features of Steel Plates with Ceramic Coating at Dynamical Three-Point Banding," *Physical Mesomechanics*, Vol. 5, No. 4, 2002, pp. 35–39.